LETTERS

Strong dipolar effects in a quantum ferrofluid

Thierry Lahaye[1], Tobias Koch[1], Bernd Fröhlich[1], Marco Fattori[1], Jonas Metz[1], Axel Griesmaier[1], Stefano Giovanazzi[1] & Tilman Pfau[1]

Symmetry-breaking interactions have a crucial role in many areas of physics, ranging from classical ferrofluids to superfluid ^{3}He and *d*-wave superconductivity. For superfluid quantum gases, a variety of new physical phenomena arising from the symmetry-breaking interaction between electric or magnetic dipoles are expected[1]. Novel quantum phases in optical lattices, such as chequerboard or supersolid phases, are predicted for dipolar bosons[2,3]. Dipolar interactions can also enrich considerably the physics of quantum gases with internal degrees of freedom[4–6]. Arrays of dipolar particles could be used for efficient quantum information processing[7]. Here we report the realization of a chromium Bose–Einstein condensate with strong dipolar interactions. By using a Feshbach resonance, we reduce the usual isotropic contact interaction, such that the anisotropic magnetic dipole–dipole interaction between ^{52}Cr atoms becomes comparable in strength. This induces a change of the aspect ratio of the atom cloud; for strong dipolar interactions, the inversion of ellipticity during expansion (the usual 'smoking gun' evidence for a Bose–Einstein condensate) can be suppressed. These effects are accounted for by taking into account the dipolar interaction in the superfluid hydrodynamic equations governing the dynamics of the gas, in the same way as classical ferrofluids can be described by including dipolar terms in the classical hydrodynamic equations. Our results are a first step in the exploration of the unique properties of quantum ferrofluids.

A quantum ferrofluid is a superfluid quantum gas consisting of polarized dipoles, either electric or magnetic. The first option (using polarized electric dipoles) might be achieved for instance with polar molecules in their vibrational ground state, aligned by an electric field. Progress has been made recently in the slowing and trapping of polar molecules (see ref. 8 and references therein), but the densities and temperatures achieved to date are far away from the quantum-degenerate regime. The use of Feshbach resonances to create polar molecules from two ultracold atomic species[9] is a promising, actively explored alternative[10]; however it is a challenging task to bring those heteronuclear molecules to their vibrational ground state[11]. Alternatively, atomic electric dipoles induced by dc fields[12] or by light[13] could be used. The second option, chosen here, relies on the magnetic dipole–dipole interaction (MDDI) between atoms with a large magnetic moment, such as chromium, for which a Bose–Einstein condensate (BEC) was achieved recently[14]. The relative strength of the MDDI to the contact interaction is conveniently expressed by the dimensionless ratio

$$\varepsilon_{\mathrm{dd}} = \frac{\mu_0 \mu^2 m}{12\pi\hbar^2 a} \qquad (1)$$

where m is the atomic mass, a is the s-wave scattering length, μ_0 is the permeability of a vacuum, $\hbar$ is $h/2\pi$, and μ is the magnetic moment (numerical factors in $\varepsilon_{\mathrm{dd}}$ are such that a homogenous BEC with $\varepsilon_{\mathrm{dd}} > 1$ is unstable against dipolar collapse). Chromium has a large dipole moment, $\mu = 6\mu_{\mathrm{B}}$, and a background scattering length in the fully polarized case of $a \approx 100\, a_0$ (μ_{B} is the Bohr magneton, and a_0 the Bohr radius), yielding[15] $\varepsilon_{\mathrm{dd}} \approx 0.16$. Although this value is typically 36 times larger than in standard alkali quantum gases, the MDDI is still a small perturbation compared to the contact interaction. A perturbative mechanical effect of the MDDI has been demonstrated by analysing the expansion of a chromium BEC from an anisotropic trap for various orientations of the dipoles[16].

The existence of Feshbach resonances[17] allows us to increase $\varepsilon_{\mathrm{dd}}$ and go beyond the perturbative limit. Indeed, close to a resonance, the scattering length varies with the applied magnetic field B as

$$a = a_{\mathrm{bg}}\left(1 - \frac{\Delta}{B - B_0}\right) \qquad (2)$$

where a_{bg} is the background scattering length, B_0 the resonance position, and Δ the resonance width. For B approaching $B_0 + \Delta$, the scattering length tends to zero, thus enhancing $\varepsilon_{\mathrm{dd}}$. This gives the possibility of reaching an MDDI-dominated quantum gas.

We report here the observation of strong dipolar effects in a chromium BEC in the vicinity of the broadest Feshbach resonance at

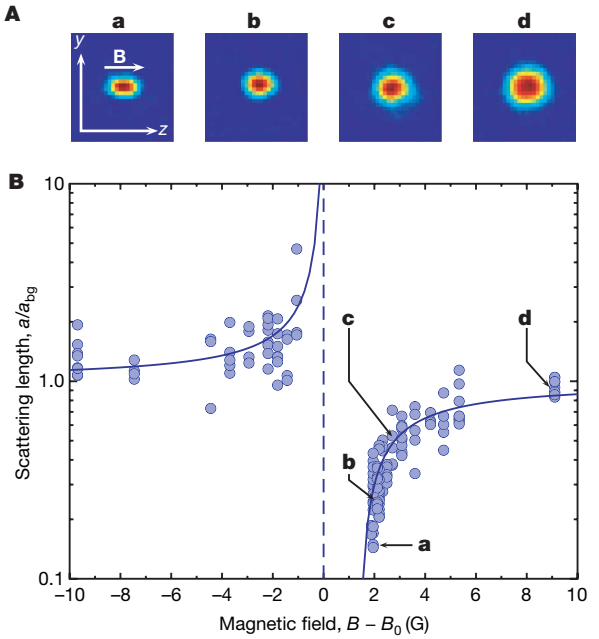

Figure 1 | Tuning the chromium scattering length. A, Absorption images (field of view 260 μm by 260 μm) of the condensate after 5 ms of expansion, for different fields B above resonance ($B - B_0$ is 2, 2.2, 2.7 and 9 G for **a**, **b**, **c** and **d**, respectively). Reducing a slows down the mean-field driven expansion. The change in aspect ratio for small a is a direct signature of strong MDDI. **B**, Variation of a across the resonance, inferred from the mean-field energy released during expansion. The line is a fit to equation (2), yielding $\Delta = 1.4 \pm 0.1$ G.

[1]5. Physikalisches Institut, Universität Stuttgart, Pfaffenwaldring 57, D-70550 Stuttgart, Germany.

$B_0 \approx 589$ G. We measure the dispersive behaviour of the scattering length, and observe that the change in a is accompanied by enhanced inelastic losses. Close to the zero-crossing of a, we observe a large modification of the aspect ratio of the cloud when ε_{dd} increases, which is direct evidence for strong dipolar effects. We finally show that the usual inversion of ellipticity of the condensate during expansion is inhibited for large enough MDDI.

We modified our experimental set-up, which has been described in detail elsewhere[14], in order to be able to produce Cr condensates in high field, close to B_0 (see Methods). Once the condensate is obtained, the magnetic field is ramped close to its final value B in 10 ms, and held there for 2 ms to let it settle down. The trap is then switched off, and the condensate expands freely for 5 ms before being imaged by absorption of resonant light in high field. Figure 1A shows a series of images taken when approaching the resonance from above, and clearly displays a reduction of the cloud size, as well as a change in its aspect ratio.

From the measured optical density profiles, we extract the BEC atom number N, as well as the Thomas–Fermi radii R_z (along the magnetization direction) and R_y (along the vertical axis). Without MDDI, one could easily obtain the scattering length a from these measurements, as the Thomas–Fermi radii after a time of flight would scale as $(Na)^{1/5}$. In our case, we take into account the MDDI using the hydrodynamic formulation of the Gross–Pitaevskii equation, including both contact and dipole–dipole interactions[18] (see Methods for the assumptions underlying our analysis). Figure 1B shows the measured variation of $a(B)$ across the resonance, showing a characteristic dispersive shape[19]. A fit according to equation (2) yields $\Delta = 1.4 \pm 0.1$ G, in good agreement with the prediction $\Delta = 1.7$ G of multi-channel calculations[17]. The position $B_0 \approx 589$ G of the resonance coincides with the one obtained by observing inelastic losses in a thermal cloud[16]. We can tune a by more than one order of magnitude, with a reduction by a factor of five above the resonance.

Close to the resonance, we observe on both sides enhanced inelastic processes resulting in a decay of the condensate. We studied the BEC atom number as a function of the time spent at the final magnetic field B, and fitted the corresponding curves by an exponential decay law (this functional form being chosen for simplicity). The 1/e BEC lifetime obtained in this way is shown in Fig. 2 as a function of B (the initial peak atomic density is 3×10^{14} cm^{-3}). Enhanced inelastic losses close to a Feshbach resonance have been observed with other species, for example, sodium[20]. Here the losses are small enough to allow us to observe the effect of the enhanced relative strength of the MDDI on the equilibrium shape of the condensate.

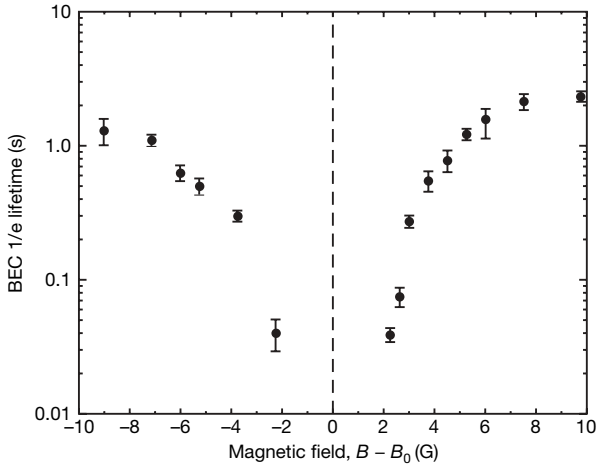

Figure 2 | Inelastic losses close to the resonance. The 1/e lifetime of the condensate is plotted as a function of the magnetic field B. Error bars correspond to one standard deviation; the lifetime was determined by fitting the atom number remaining in the BEC after a variable holding time with an exponential decay law. The losses are small enough to allow for the observation of enhanced dipolar interactions (see Methods).

Figure 3 shows the aspect ratio R_y/R_z of the cloud as a function of the value of ε_{dd} obtained from the measured a, and constitutes the main result of this Letter. The aspect ratio decreases when ε_{dd} increases: the cloud becomes more elongated along the direction of magnetization z, as can be seen unambiguously in Fig. 1A. This is a clear signature of the MDDI, as for pure contact interaction, the aspect ratio is independent of the scattering length (provided the Thomas–Fermi approximation is valid). The solid line in Fig. 3 shows the aspect ratio after time of flight calculated using the hydrodynamic theory including MDDI[18], without any adjustable parameter. The agreement between our data and the theoretical prediction is excellent, given the dispersion of data points and the uncertainty in the theoretical prediction arising from the measurements of trap frequencies. The highest value of ε_{dd} we could reach reliably is about 0.8, corresponding to a fivefold reduction of the scattering length. For our trap geometry, the condensate is expected to become unstable with respect to dipolar collapse[21,22] for values of ε_{dd} slightly above one (the exact value depending on the trap anisotropy, but also on the atomic density).

As an application of the tunability of the dipolar parameter, we study the expansion of the condensate for two orthogonal orientations of the dipoles with respect to the trap, as was done in ref. 16, but now as a function of ε_{dd}. In practice, for the large fields required to approach the Feshbach resonance, we cannot change the magnetic field orientation, which is always along z. We therefore use two different trap configurations, with interchanged y and z frequencies, and identical frequencies along x: trap 1 has frequencies $(\omega_x,\omega_y,\omega_z)/2\pi \approx (660,370,540)$ Hz, while trap 2 has $(\omega_x,\omega_y,\omega_z)/2\pi \approx (660,540,370)$ Hz. We then measure the aspect ratio of the cloud (defined as $A_1 = R_z/R_y$ for trap 1, and $A_2 = R_y/R_z$ for trap 2) as a function of the time of flight, for different values of B (and hence of ε_{dd}). This protocol is equivalent to a mere rotation of the magnetization direction with respect to the trap axes.

Figure 4 presents the results. In order to check that the two trap configurations only differ by an exchange of the y and z frequencies, we first perform the expansion experiment without switching on the

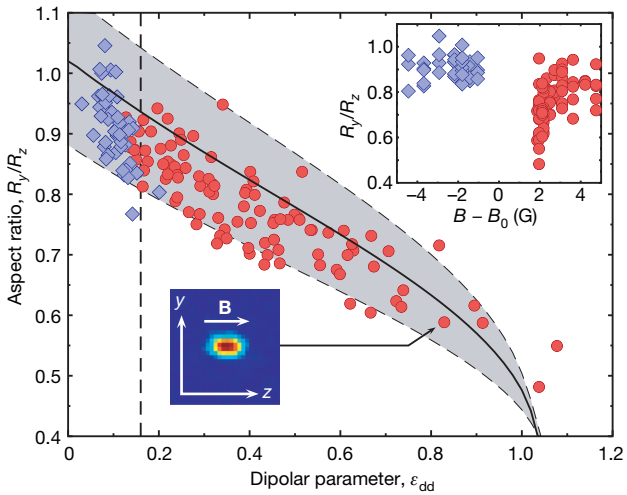

Figure 3 | Increasing the dipolar parameter. Main plot, condensate aspect ratio after 5 ms of expansion plotted against the measured ε_{dd}. Diamonds (circles) correspond to data taken below (above) resonance. The solid line is the prediction of hydrodynamic theory including MDDI, without adjustable parameters (the grey-shaded area corresponds to the uncertainties in the trap frequencies). The dashed line indicates the off-resonant ε_{dd} value. Top right inset, a subset of the same data points plotted against the magnetic field. The condensate elongates appreciably along B only just above resonance, when a approaches zero. Bottom left inset, sample absorption image giving an example of a condensate with strong MDDI.

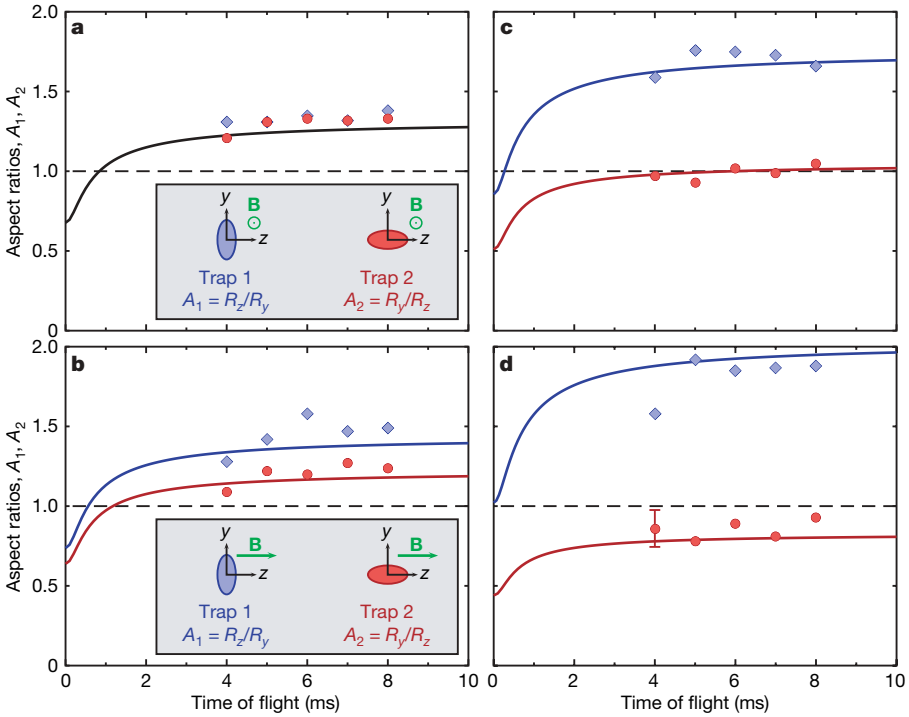

Figure 4 | MDDI-dominated BEC expansion. Aspect ratio of the condensate versus time of flight, for two traps with interchanged y and z frequencies (see text). The solid lines are theoretical predictions without adjustable parameters. The error bar (in **d**) gives the typical dispersion over several runs. **a**, Dipoles perpendicular to the observation plane (see inset sketching the in-trap BEC shape); both configurations yield the same aspect ratio. **b**–**d**, Dipoles along z (see inset in **b**); ε_{dd} takes the values 0.16 (**b**), 0.5 (**c**) and 0.75 (**d**). The MDDI induces larger and larger effects, even inhibiting (**d**) the inversion of ellipticity.

large magnetic field along z, but with a small (11.5 G) field along x (the line of sight of the imaging). The magnetization is therefore perpendicular to the observation plane, and changing the trap configuration does not affect the aspect ratios, as the difference between the two situations is simply a rotation of the trap around the magnetization axis. Figure 4a shows the equality $A_1 = A_2$, confirming the equivalence of the two configurations. We then study the expansion with the large magnetic field B along z. In this case, the MDDI induces a change in the aspect ratios, and $A_1 \neq A_2$. Far from resonance, $\varepsilon_{dd} \approx 0.16$ and we recover the perturbative dipolar effect already observed in ref. 16 (see Fig. 4b). However, for values of B approaching $B_0 + \Delta$, ε_{dd} increases and, correspondingly, the difference between A_1 and A_2 becomes very large (Fig. 4c and d, where ε_{dd} is 0.5 ± 0.1 and 0.75 ± 0.1, respectively). The lines correspond to the prediction of the hydrodynamic theory without adjustable parameters, and show again a very good agreement with the data. The effect of the dipolar interaction is far beyond the perturbative regime, and induces very strong deviations from what one expects for contact interaction. In particular, for $\varepsilon_{dd} \approx 0.75$, the aspect ratio A_2 always remains smaller than unity during the time of flight: the strong anisotropic dipolar interaction inhibits the inversion of ellipticity, the 'smoking gun' evidence for BECs with contact interaction.

In conclusion, the use of a Feshbach resonance to reduce the s-wave scattering length of chromium allowed us to realize a BEC with strong dipolar interaction, and to study the hydrodynamics of this novel quantum ferrofluid. This work opens up many avenues towards the study of dipolar quantum gases beyond the perturbative regime. Structured density profiles are predicted for dipolar condensates in anisotropic traps[23], including biconcave density distributions in pancake-shaped traps[24]. A clear direction for future work is thus to use a one-dimensional optical lattice, creating a stack of pancake-shaped traps. A condensate with dipoles perpendicular to the trap plane is then stable with respect to dipolar collapse, which should allow entry to the regime $\varepsilon_{dd} \gg 1$. In particular, the investigation of the unusual, roton-like excitation spectrum predicted in this system[25] is a fascinating possibility. The creation of Cr_2 molecules by ramping over the Feshbach resonance is another appealing experiment. In a two-dimensional trap, the repulsive interaction between the molecules, due to their large magnetic moment, might stabilize them against inelastic losses. Another possible extension of this work is the study of degenerate fermions with strong dipolar interactions, which may display new types of pairing mechanisms (ref. 1, and references therein). Finally, the behaviour of strongly correlated dipolar quantum gases in three-dimensional optical lattices is an interesting open field, with many connections to fundamental questions in condensed-matter physics—such as the study of supersolid phases, whose experimental observation in helium is still debated (see, for example, ref. 26).

METHODS SUMMARY

We modified our experimental sequence[14] to produce chromium condensates in high field. For this, we switch on quickly (in less than 5 ms) a large field (~600 G) during forced evaporation in the dipole trap. The low atomic density at this stage of evaporation allows for small losses. The current in the coils used to produce the field is actively stabilized; care is taken to ensure a high homogeneity of the field. Evaporation is then resumed until an almost pure condensate of 3×10^4 atoms is obtained. The trap is then adjusted to obtain frequencies $(\omega_x,\omega_y,\omega_z)/2\pi \approx (840,600,580)$ Hz (measured by exciting the centre of mass motion of the cloud, with an accuracy of 5%).

In our data analysis to extract the scattering length a (Fig. 1), we assumed that no external forces act on the atoms during the time of flight, that the condensate stays in equilibrium during the magnetic field ramp, and finally that the hydrodynamic (Thomas–Fermi) approximation is valid even for small a. These assumptions are largely fulfilled for all our parameters.

Full Methods and any associated references are available in the online version of the paper at www.nature.com/nature.

Received 4 May; accepted 15 June 2007.

1. Baranov, M., Dobrek, Ł., Góral, K., Santos, L. & Lewenstein, M. Ultracold dipolar gases — a challenge for experiments and theory. *Phys. Scr.* **T102**, 74–81 (2002).

2. Góral, K., Santos, L. & Lewenstein, M. Quantum phases of dipolar bosons in optical lattices. *Phys. Rev. Lett.* **88,** 170406 (2002).
3. Menotti, C., Trefzger, C. & Lewenstein, M. Metastable states of a gas of dipolar bosons in a 2D optical lattice. *Phys. Rev. Lett.* **98,** 235301 (2007).
4. Kawaguchi, Y., Saito, H. & Ueda, M. Einstein–de Haas effect in dipolar Bose-Einstein condensates. *Phys. Rev. Lett.* **96,** 080405 (2006).
5. Santos, L. & Pfau, T. Spin-3 chromium Bose-Einstein condensates. *Phys. Rev. Lett.* **96,** 190404 (2006).
6. Yi, S. & Pu, H. Spontaneous spin textures in dipolar spinor condensates. *Phys. Rev. Lett.* **97,** 020401 (2006).
7. DeMille, D. Quantum computation with trapped polar molecules. *Phys. Rev. Lett.* **88,** 067901 (2002).
8. Doyle, J., Friedrich, B., Krems, R. V. & Masnou-Seeuws, F. (eds) Special issue on ultracold molecules. *Eur. Phys. J. D* **31,** 149–445 (2004).
9. Köhler, T., Góral, K. & Julienne, P. S. Production of cold molecules via magnetically tunable Feshbach resonances. *Rev. Mod. Phys.* **78,** 1311–1361 (2006).
10. Ospelkaus, C. *et al.* Ultracold heteronuclear molecules in a 3D optical lattice. *Phys. Rev. Lett.* **97,** 120402 (2006).
11. Sage, J., Sainis, S., Bergeman, T. & DeMille, D. Optical production of ultracold polar molecules. *Phys. Rev. Lett.* **94,** 203001 (2005).
12. Marinescu, M. & You, L. Controlling atom-atom interaction at ultralow temperatures by dc electric fields. *Phys. Rev. Lett.* **81,** 4596–4599 (1998).
13. Giovanazzi, S., O'Dell, D. & Kurizki, G. Density modulations of Bose-Einstein condensates via laser-induced interactions. *Phys. Rev. Lett.* **88,** 130402 (2002).
14. Griesmaier, A., Werner, J., Hensler, S., Stuhler, J. & Pfau, T. Bose-Einstein condensation of chromium. *Phys. Rev. Lett.* **94,** 160401 (2005).
15. Griesmaier, A. *et al.* Comparing contact and dipolar interactions in a Bose-Einstein condensate. *Phys. Rev. Lett.* **97,** 250402 (2006).
16. Stuhler, J. *et al.* Observation of dipole-dipole interaction in a degenerate quantum gas. *Phys. Rev. Lett.* **95,** 150406 (2005).
17. Werner, J., Griesmaier, A., Hensler, S., Stuhler, J. & Pfau, T. Observation of Feshbach resonances in an ultracold gas of ^{52}Cr. *Phys. Rev. Lett.* **94,** 183201 (2005).
18. Giovanazzi, S. *et al.* Expansion dynamics of a dipolar Bose-Einstein condensate. *Phys. Rev. A* **74,** 013621 (2006).
19. Inouye, S. *et al.* Observation of Feshbach resonances in a Bose-Einstein condensate. *Nature* **392,** 151–154 (1998).
20. Stenger, J. *et al.* Strongly enhanced inelastic collisions in a Bose-Einstein condensate near Feshbach resonances. *Phys. Rev. Lett.* **82,** 2422–2425 (1999).
21. Santos, L., Shlyapnikov, G. V., Zoller, P. & Lewenstein, M. Bose-Einstein condensation in trapped dipolar gases. *Phys. Rev. Lett.* **85,** 1791–1794 (2000).
22. Góral, K., Rzążewski, K. & Pfau, T. Bose-Einstein condensation with magnetic dipole-dipole forces. *Phys. Rev. A* **61,** 051601(R) (2000).
23. Dutta, O. & Meystre, P. Ground-state structure and stability of dipolar condensates in anisotropic traps. *Phys. Rev. A* **75,** 053604 (2007).
24. Ronen, S., Bortolotti, D. C. E. & Bohn, J. L. Radial and angular rotons in trapped dipolar gases. *Phys. Rev. Lett.* **98,** 030406 (2007).
25. Santos, L., Shlyapnikov, G. V. & Lewenstein, M. Roton-maxon spectrum and stability of trapped dipolar Bose-Einstein condensates. *Phys. Rev. Lett.* **90,** 250403 (2003).
26. Sasaki, S., Ishiguro, R., Caupin, F., Maris, H. J. & Balibar, S. Superfluidity of grain boundaries and supersolid behavior. *Science* **313,** 1098–1100 (2006).

Acknowledgements We thank L. Santos for discussions and J. Stuhler for contributions in the initial phases of the experiment. We acknowledge financial support by the German Science Foundation (SFB/TRR21) and the EU (Marie-Curie fellowship to T.L.).

Author Information Reprints and permissions information is available at www.nature.com/reprints. The authors declare no competing financial interests. Correspondence and requests for materials should be addressed to T.L. (t.lahaye@physik.uni-stuttgart.de) or T.P. (t.pfau@physik.uni-stuttgart.de).

METHODS

Production of Cr condensates in a high magnetic field. We load chromium atoms in the $|^7S_3, m_S = 3\rangle$ state into a Ioffe magnetic trap for 10 s, and subsequently cool them by r.f.-induced evaporation down to 20 μK. We capture 10^6 of these atoms in an optical trap consisting of a horizontal laser beam at 1,076 nm with a power of 16 W and a $1/e^2$ radius of 30 μm, and optically pump them in the high-field seeking state $|m_S = -3\rangle$. A 11.5 G magnetic field prevents losses due to dipolar relaxation. At this stage, a vertical beam (power 9 W, $1/e^2$ radius 50 μm) is ramped up over 5 s, creating a 'dimple' in the trap. We then ramp the horizontal beam power down to 30% of its initial value in 5 s, and switch on rapidly (less than 5 ms) a magnetic field B_{evap} along z. The field is provided by the offset and pinch coils of the Ioffe trap, in which we run currents of around 400 A and 15 A, respectively. This combination ensures that the field is as homogenous as possible. The remaining inhomogeneities correspond to trapping (anti-trapping) frequencies below 5 Hz (7 Hz) radially (longitudinally). The current in the offset coils is stabilized at the 3×10^{-5} level (r.m.s.), giving in principle a control of the field better than 100 mG. B_{evap} is 600 G (575 G) for the data taken above (below) resonance. The fast magnetic ramp and the low atomic density (about 10^{13} cm^{-3}) at this stage of the evaporation are required to cross the resonances below B_{evap} without appreciable losses. Forced evaporation is resumed in high field until an almost pure condensate of 3×10^4 atoms is obtained. The powers of the beams are finally adjusted adiabatically to reach the desired trap frequencies.

Data analysis for the measurement of *a*. The assumptions in our analysis are: (1) no external forces act on the atoms during the expansion; (2) the condensate stays in equilibrium during the magnetic field ramp; and (3) the hydrodynamic (Thomas–Fermi) approximation is valid. We therefore checked (1) that the effect of the inhomogeneities of the magnetic field during expansion is completely negligible for our parameters, and (2) that the magnetic field ramp is slow enough to fulfil the adiabaticity criterion $\dot{a}/a \ll \omega_{min}$, where ω_{min} is the smallest trap frequency. We checked that no collective oscillations were excited in the condensate when varying a. For this, we varied the time spent at the final magnetic field B before expansion, and observed no change in the condensate shape, even for the data taken close to $B_0 + \Delta$. Note that the occurrence of losses makes the adiabaticity criterion more difficult to fulfil, as one must stay far enough from resonance in order to satisfy $\dot{N}/N \ll \omega_{min}$. This criterion is largely fulfilled for our data. Finally, we checked (3) that the hydrodynamic description of the condensate is valid: the Thomas–Fermi parameter, defined as Na/a_{ho}, where $a_{ho} = \sqrt{\hbar/(m\bar{\omega})}$ is the trap harmonic oscillator length and $\bar{\omega} = (\omega_x\omega_y\omega_z)^{1/3}$, is always higher than ~60 (a value achieved for the lowest values of a and N). The Thomas–Fermi condition $Na/a_{ho} \gg 1$ is therefore fulfilled.